

Concerning the Multiscale Structure of Solar Convection

A. V. Getling^a, O. S. Mazhorova^b, and O. V. Shcheritsa^b

^a *Skobeltsyn Institute of Nuclear Physics, Moscow State University, Moscow, 119991 Russia*
e-mail: A.Getling@mail.ru

^b *Keldysh Institute of Applied Mathematics, Moscow, 125047 Russia*
e-mail: olgamazhor@mail.ru, shchery@mail.ru

Received April 25, 2013

Abstract—The discrete scale spectrum of the convective flows observed on the Sun has not yet received a convincing explanation. Here, an attempt is made to find conditions for the coexistence of convective flows on various scales in a horizontal fluid layer heated from below, where the thermal diffusivity varies with temperature in such a way that the static temperature difference across a thin sublayer near the upper surface of the layer is many times larger than the temperature variation across the remainder of the layer. The equations of two-dimensional thermal convection are solved numerically in an extended Boussinesq approximation, which admits thermal-diffusivity variations. The no-slip conditions are assumed at the lower boundary of the layer; either no-slip or free-slip conditions, at the upper boundary. In the former case, stable large-scale rolls develop, which experience small deformations under the action of small structures concentrated near the horizontal boundaries. In the latter case, the flow structure is highly variable, different flow scales dominate at different heights, the number of large rolls is not constant, and a sort of intermittency occurs: the enhancement of the small-scale flow component is frequently accompanied by the weakening of the large-scale one, and vice versa. The scale-splitting effects revealed here should manifest themselves in one way or another in the structure of solar convection.

DOI: 10.1134/S0016793213070074

1. INTRODUCTION

At least four types of cellular structures, strongly differing in their scale, can be identified with certainty on the solar surface and attributed to the phenomenon of thermal convection, i.e., granules, mesogranules, supergranules, and giant cells. They may not exhaust all existing types: in particular, there are indications for the presence of “large mesogranules”, i.e., cells intermediate in their scale between supergranules and mesogranules (Getling and Buchnev, 2010). This multiscale structure is an important feature of solar convection, which should be taken into account in studying the dynamics of magnetic fields. It has not yet received a convincing explanation, and an adequate hydrodynamic description must be given to both the spatial structure of the flows and the factors responsible for its development.

As is known, convection cells that are not large in their plan size compared to the full thickness of the convecting-fluid layer should also be vertically localized in a relatively thin portion of this layer. This is obviously possible if a certain sublayer (height interval) where convection can develop due to an unstable temperature stratification, is contiguous with another sublayer where the stratification is stable and exerts a braking action on the convective motion (in this case, the flow nevertheless penetrates into the stable region; i.e., penetrative convection occurs). If, however, the

entire layer (from top to bottom) is convectively unstable, the localization of motion in a relatively thin sublayer is not such a trivial effect. The possibility of the coexistence of small cells with larger ones, filling the entire layer thickness, is even less obvious.

The aim of this study is to understand whether or not the particularities of the static temperature stratification of a fluid layer unstable at all heights can give rise to a multiscale spatial spectrum of convection. It can be naturally suggested that scale splitting could result from sharp changes in the vertical entropy gradient (or the temperature gradient in the case of an incompressible fluid) at some heights. Under the conditions of the solar convection zone, there are some prerequisites for manifestations of such an effect, related to the enhanced instability of the sublayers of partial ionization of hydrogen and helium. Indirect indications for the possible scale splitting in such situations were found previously in linear problems (Getling, 1975; Getling, 1980), and these expectations were substantiated in part by nonlinear numerical computations (Getling and Tikhomolov, 2007).

2. FORMULATION OF THE PROBLEM AND SOLUTION PROCEDURE

We investigate here possibilities of scale splitting in the case where the static temperature gradient experiences a sharp change at a certain height, by means of

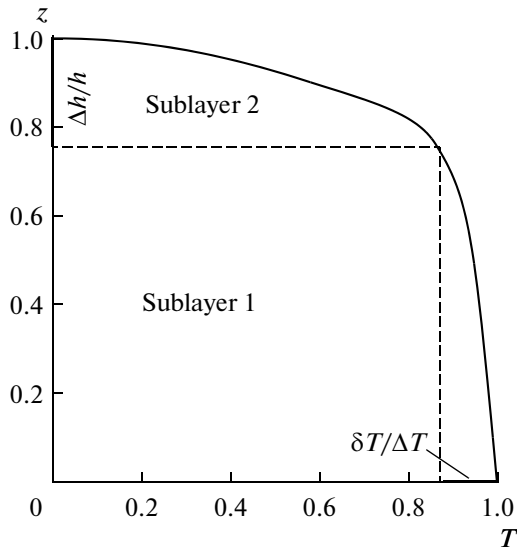


Fig. 1. Static temperature profile (in nondimensional variables) for $a = 20$, $b = 600$, and $n = 20$.

numerically simulating two-dimensional convection flows in a plane horizontal incompressible-fluid layer (of thickness h) heated from below. We assume that the temperature difference between the bottom and top surfaces of the layer is ΔT and specify the temperature dependence of the thermal diffusivity in the form $\chi(T) = 1 + aT + bT^n$. We choose parameters a , b , and n in such a way that temperature varies little (by $\delta T \ll \Delta T$) across the main portion of the layer of thickness $h - \Delta h$, $\Delta h \ll h$ (sublayer 1); the most part of the temperature difference, $\Delta T - \delta T$, corresponding to sublayer 2 with small thickness Δh near the upper surface (Fig. 1).

The horizontal size of our computational domain is $5\pi h = 15.7h$. The no-slip impermeability conditions are specified at the bottom and side boundaries of the domain. The top boundary may be either rigid or stress-free. The temperature is fixed at the horizontal boundaries, and the heat flux vanishes at the sidewalls. The flow is initialized by introducing a random thermal perturbation at a certain height within the upper sublayer.

The process is characterized by nondimensional parameters termed the Rayleigh and Prandtl numbers

$$R = \frac{\alpha g \Delta T h^3}{\nu \chi}, \quad P = \frac{\nu}{\chi},$$

where α is the volumetric coefficient of thermal expansion of the fluid; ν and χ are its kinematic viscosity and thermal diffusivity (the value of the latter being taken at the upper boundary of the layer); and g is the gravitational acceleration. We also introduce the “local” Rayleigh numbers R_1 and R_2 for the lower (first) and upper (second) sublayers, respectively, according to their thicknesses and temperature differences. In an extended Boussinesq approximation, which admits thermal-diffusivity variations, we solve the system of Navier–Stokes equations, written for the stream function and vorticity, using a finite-difference technique. We employ a conservative scheme of the second-order accuracy in the spatial coordinates and of the first order in time (Mazhorova and Popov, 1980). Calculations are carried out on a nonuniform grid, which is finer near the top and bottom layer boundaries. The total number of nodes is 1024×51 .

In the regimes studied, the critical Rayleigh number, which was determined in the process of simulation of convection, was in the range $R_c = (4 - 6) \times 10^5$ for the layer with a rigid (no-slip) upper boundary and equal to $R_c \approx 3.8 \times 10^6$ for the layer with a free-slip upper surface; the Prandtl number in our calculations was in the range $P = 0.01 - 10$. A temperature profile of the form of interest was obtained at $b = 600$, $a = 10 - 20$, and $n = 10 - 20$; $R_1 > R_2$ for the considered static temperature profile. The qualitative features of the results turned out to be little sensitive to the choice of parameters a and n in the above-mentioned ranges.

3. RESULTS

If the upper horizontal boundary is rigid, then motion starts developing in the form of small-scale convection in the upper sublayer (2), for which the conventionally defined local Rayleigh number is smaller than for sublayer 1 and which is thus more stable according to formal criterion $R_2 < R_1$. Later, the disturbances penetrate deeper and gradually involve the entire layer depth. As a result, large-scale roll cells emerge with a width of about the layer thickness, while small-scale cells are observed both in the upper sublayer and near the lower layer boundary. Thus, in the fluid layer stratified, on the whole, unstably, large cells filling the entire layer depth coexist with smaller ones localized in relatively thin sublayers (Fig. 2). The small cells are especially pronounced above the contact sections of large rolls. We investigated the structure of the developing flow using an ideal low-pass filter based on a two-dimensional Fourier transform, which was



Fig. 2. Coexistence of large cells and a smaller-scale flow at $R \approx 10R_c$ and $P = 1$ in the case of a rigid upper boundary; $a = 20$, $n = 20$. Streamlines (contours of the stream function) are shown.

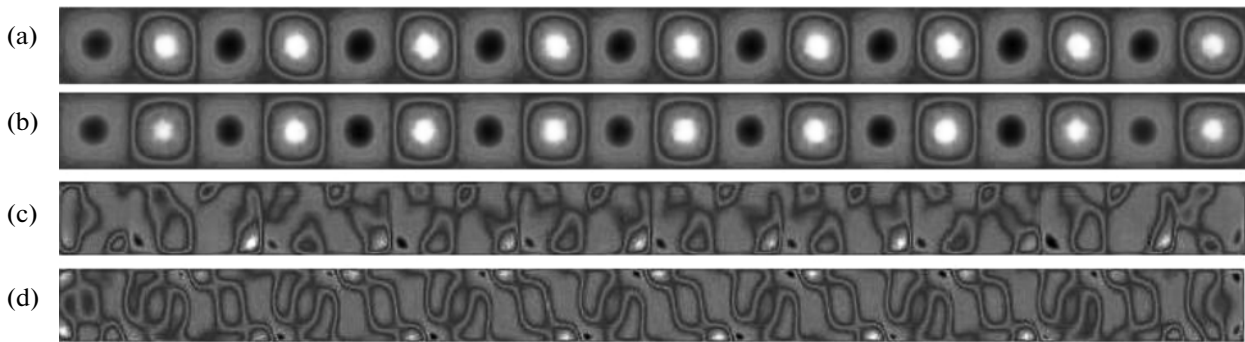


Fig. 3. (a) Flow pattern (stream-function distribution) computed for $R \approx 10R_c$ and $P = 10$ and typical of the case of a rigid upper boundary; (b) large-scale structures separated from this field using a low-pass filter; (c) small-scale structures obtained by subtracting the large-scale component from the full stream-function field for $P = 10$; and (d) similar small-scale structures at $P = 0.5$.

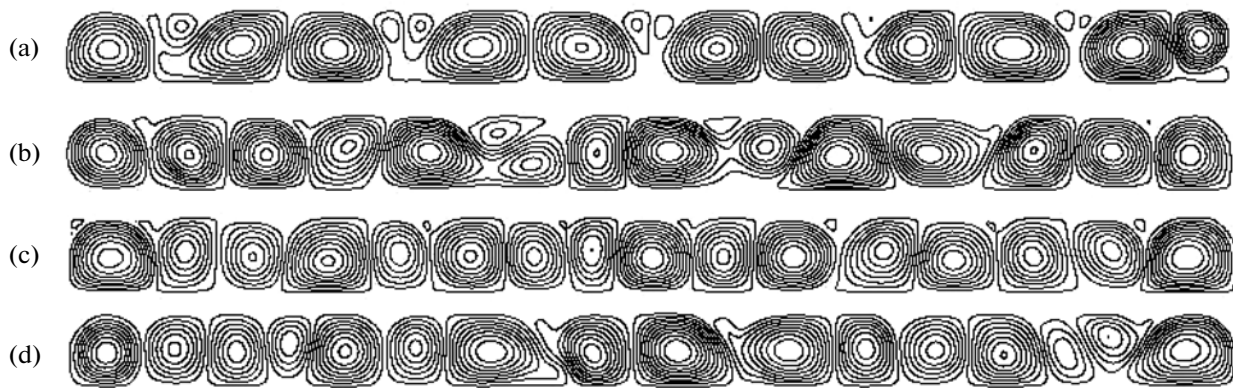


Fig. 4. Flow evolution in the case of a free upper boundary ($R \approx 1.5R_c$ and $P = 1$). Streamlines (contours of the stream function) are shown for various times: (a) $t = 0.07t_v$, small-scale cells emerge near the upper layer boundary; (b) $t = 0.09t_v$, a “breaking” effect of the small cells penetrating deep down on the large rolls with horizontal sizes considerably exceeding the scale optimum; (c) $t = 0.14t_v$, flow pattern formed due to the penetration of small-scale cells deep into the layer; (d) $t = 0.17t_v$, a tendency towards increases in the size of large-scale cells; emergence and development of small-scale structures in the upper sublayer is noticeable in (c) and (d).

applied to the stream function to separate the large-scale component of the flow. The subtraction of the large-scale component from the full field separated the small-scale flow component, thus visualizing small cellular structures; the smaller the Prandtl number, the more pronounced they are (Fig. 3).

In the case of a free upper boundary, the flow also starts evolving in the upper sublayer, after which the emerged small-scale structures penetrate deeper into the layer, stimulating the development of a flow throughout the layer. The cells in sublayer 1 tend to grow in size; however, the small-scale structures present in sublayer 2 control this process: as the horizontal size of a large structure becomes considerably larger than the layer thickness, the cells moving down from the upper sublayer break this structure into two portions (Fig. 4). In contrast to the case of a rigid upper boundary, where the number of large rolls is

constant, the number of large-scale structures in the layer with the free boundary varies between 8 and 16. Analyses of the spectra obtained by the Fourier decomposition of the stream function in the horizontal coordinate have shown that harmonics with different wavenumbers dominate at different heights. Figure 5 shows a set of flow spectra for the times $t = 0.14t_v$ and $0.17t_v$ at $R \approx 1.5R_c$, $P = 1$; here, t_v is the time of viscous dissipation on scale h . Harmonics with the wavenumbers $k = 2.8$ and 3.2 dominate in the bulk of the layer, while a harmonic with $k = 4$ dominates in the upper sublayer (the nondimensional form of the wavenumber that we use corresponds to the wavelength measured in units of h). The sublayers where the small cells are located vary their thicknesses and do not coincide with sublayers 1 and 2, specified by the static vertical temperature profile. In contrast to the case of a rigid

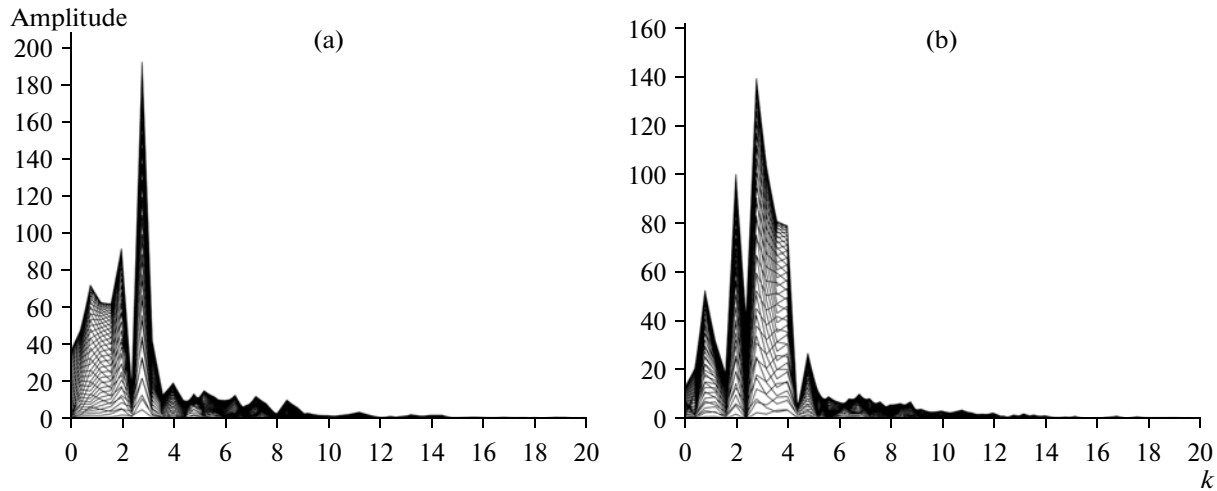


Fig. 5. Amplitude spectra of the stream function obtained in a run with a free upper boundary at $R \approx 1.5R_c$ and $P = 1$ for the times $t = 0.14t_v$ (a) and $0.17t_v$ (b). Different curves correspond to different heights.

upper boundary, the small-scale structures are only located in the upper portion of the layer.

A consideration of the spectrum of the stream function averaged over the layer thickness has shown that the amplitudes of the harmonics in the case of a rigid upper boundary remain virtually unchanged, and the same harmonic always dominates. A qualitatively different situation takes place if the upper boundary is free. In this case, both the spatial pattern of the flow and the spectra are highly variant, and the amplitudes of different harmonics at a given height and their ratios fluctuate so that harmonics with different wavenumbers dominate at different times. The enhancement of the small-scale component is frequently accompanied

by the weakening of the large-scale component and vice versa: a type of intermittency is observed (Fig. 6).

4. CONCLUSIONS AND DISCUSSION

Clearly, the simplified model considered here cannot offer a realistic description of solar convection, the structure of which depends on a multitude of factors, such as the density difference across the convection zone, the complex thermal stratification, the complex equation of the state of the matter (related to the variable ionization degree), radiative heat exchange, etc. Nevertheless, such models are instructive in terms of evaluating the possible role of various factors in the formation of the real pattern.

In this case, we can see that the stratification due to the variable thermal diffusivity, if the static temperature profile has a sharp kink, can give rise to the development of small-scale flows and, on the whole, to the splitting of convection scales. In the case of two rigid boundaries, small-scale cells are localized in both the upper and bottom boundary sublayers. However, small-scale cells are only observed near the upper boundary, if it is free. Then, harmonics with different wavenumbers dominate at different heights, and a type of intermittency takes place: the enhancement of the small-scale component is frequently accompanied by the weakening of the large-scale component and vice versa; on the whole, the flow pattern in the layer with a free upper boundary is far from stationary. In both cases, the thickness of the localization zones of small-scale cells exceeds the thickness of the sublayer with a sharp temperature change (Δh). Small cells are transferred by large-scale flows; if the upper boundary is free, this process appears as the sinking of small cells.

An improvement of this model could likely make it possible to comprehend the structure of solar convec-

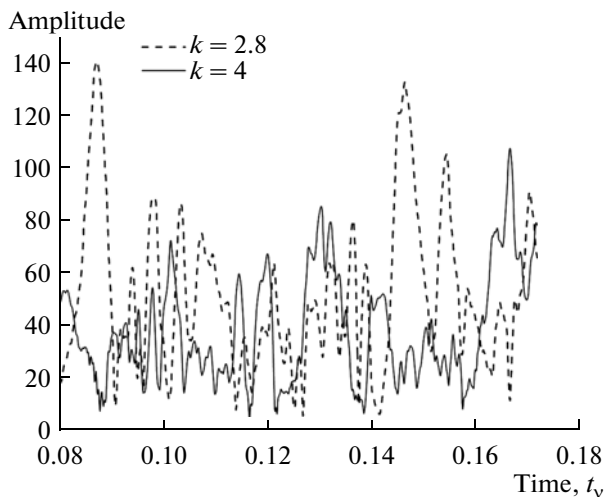


Fig. 6. Time variation in the amplitudes of harmonics with wavenumbers $k = 2.8$ and 4 in a run with a free upper boundary and $R \approx 1.5R_c$, $P = 1$.

tion. In particular, a step in this direction could be the consideration of a model in which the upper boundary is replaced with a stable sublayer overlying unstable sublayer 2.

ACKNOWLEDGMENTS

This work was supported by the Russian Foundation for Basic Research, project no. 12-02-00792-a.

REFERENCES

- Getling, A.V., Convective motion concentration at the boundaries of a horizontal fluid layer with inhomogeneous unstable temperature gradient along the height, *Fluid Dyn.* 1976, vol. 10, pp. 745–750.
- Getling, A.V., Scales of convective flows in a horizontal layer with radiative transfer, *Izv., Atmosph. Oceanic Phys.*, 1980, vol. 16, no. 5, pp. 363–365.
- Getling, A.V. and Buchnev, A.A., Some structural features of the convective-velocity field in the solar photosphere, *Astron. Rep.*, 2010, vol. 54, pp. 254–259.
- Getling, A.V. and Tikhomolov, E.M., Scale splitting in solar convection, *Trudy XI Pulkovskoi mezhdunarodnoi konferentsii po fizike Solntsa* (Proc. 11th Pulkovo Int. Conf. on Solar Physics), Pulkovo, 2007, pp. 109–112.
- Mazhorova, O.S. and Popov, Yu.P., Methods for the numerical solution of the Navier–Stokes equations, *USSR Comput. Math. Math. Phys.*, 1980, vol. 20, no. 4, pp. 202–217.

Translated by A. Getling